# Enhancement in Crystallinity of Poly(3-hexylthiophene) Thin Films Prepared by Low-Temperature Drop Casting

**Thankaraj Salammal Shabi,[1] Souren Grigorian,[1] Martin Brinkmann,[2] Ullrich Pietsch,[1] Nils Koenen,[3] Navaphun Kayunkid,[2] Ullrich Scherf[3]**

[1]*Solid State Physics, University of Siegen, Walter Flex Strasse-3, D-57068 Siegen, Germany*
[2]*Institute Charles Sadron, CNRS-University of Strasbourg, 23 rue du loess, 67034 Strasbourg, France*
[3]*Macromolecular Chemistry, University of Wuppertal, D-42097, Gauss-Str.20, Wuppertal, Germany*

Received 15 July 2011; accepted 7 November 2011
DOI 10.1002/app.36447
Published online 22 January 2012 in Wiley Online Library (wileyonlinelibrary.com).

**ABSTRACT:** Low-temperature casting of high molecular weight (HMW > 40 kDa) regioregular poly(3-hexylthiophene) (P3HT) is demonstrated to yield highly crystalline P3HT thin films with well defined and preferentially edge-on oriented [(100) contact plane] nanocrystallites on the pure and silanized $Si/SiO_2$ substrates. Transmission electron microscopy and X-ray diffraction provide evidence for the increase in preferential edge-on orientation of P3HT-conjugated backbone while decreasing the film preparation temperature below room temperature. The optimum growth temperature is about −12°C for the given concentration (2 mg/mL in $CHCl_3$). The reduced evaporation rate of the solvent results in a better selection of the thermodynamically stable orientation of nanocrystallites onto the substrate. The degree of preferential orientation and size of the crystallites can be further increased on *n*-octadecyltrichlorosilane-treated $SiO_2$ substrates as well as by annealing the films at 200°C for 1 h. © 2012 Wiley Periodicals, Inc. J Appl Polym Sci 125: 2335–2341, 2012

**Key words:** conjugated semiconducting polymers; GIXD; TEM; thin film structure; P3HT

## INTRODUCTION

Conjugated polymers such as regioregular poly(3-alkylthiophene)s (P3ATs) have attracted much attention in the electronic industries due to their unique charge transport properties with high charge-carrier mobilities in the range $10^{-1}$–$10^{-3}$ $cm^2/Vs$ and ease of processability due to their solubility in organic solvents.[1] P3AT thin films can be prepared by various deposition methods, e.g., spin-coating, solution casting, and deposition by doctor blade technique or ink jet printing.[1,2] Among the P3AT family, poly(3-hexylthiophene) (P3HT) is now the working horse for the fabrication of organic thin film transistors (OFETs) and organic solar cells.[3,4] Nowadays, it is rather well established that the crystallinity and nanomorphology of the P3HT films impact the charge transport properties.[5–8] This is essentially due to (i) the semicrystalline character of P3HT, i.e., amorphous and crystalline domains coexist in thin films[9] and (ii) the charge transport is highly anisotropic in conjugated polymers.[6,8] Structurewise, P3AT shows a characteristic "lamellar" ordering into layers of π−π−stacked conjugated backbones separated by about 0.38 nm.[7,9] The period of more or less ordered side chains lies between 1.55 and 1.67 nm, depending on the overall ordering and molecular weight of polymer. Typically, the unit cell of P3HT is chosen in such a way that the side chains are directed along the *a*-axis, the π–π-stacking along the *b*-axis, and the main chain direction along the *c*-axis. The favorable orientation of P3HT nanocrystallites in an OFET is such that both the *c* and *b* axes lie in the plane of the substrate, i.e., nanocrystals have a preferential (100) contact plane also called "edge-on" orientation as opposed to the "face-on" orientation corresponding to the preferential (010) contact plane.[7]

Several strategies have been followed to favor the preferential edge-on orientation of the crystalline domains.[5–7,9,10] Sirringhaus et al.[10] have shown that the use of a high boiling point solvent like 1,2,4-trichlorobenzene (TCB) favors the edge-on orientation of P3HT crystalline domains. In the case of spin-coated films, the use of self-assembled monolayers is an elegant way to promote the edge-on orientation.[5,11] Three well-known techniques such as spin-coating, printing, and casting (doctor blade) are widely used in industry for the fabrication of large

Additional Supporting Information may be found in the online version of this article.

*Correspondence to:* S. Grigorian (grigorian@physik.uni-siegen.de).

Contract grant sponsors: DAAD (German Academic Exchange Service) (T.S. Shabi).

scale devices.[2] Films prepared by doctor blade (casting) and spin coating often show face-on oriented crystallites[5,11,12] which are not favorable for the in-plane charge transport in an OFET device.[6,8] However, spin coating is a process that results in thin film morphologies far from the equilibrium conditions. The postgrowth annealing treatment has been widely applied to the spin coated P3HT films because of the formation nonthermodynamically stable crystallites due to the complex interplay of solvent evaporation and molecular aggregation.[5,6,11] It can reduce the internal stress, defects, and the polymer chains become more mobile, so they can self-organize in a most thermodynamically stable state.[13] The *in situ* annealing analysis performed for the P3HT film shows two different results: (i) the increase in annealing temperature enhances the edge-on oriented crystallites and (ii) it cause expansion of the (h00) planes and compression of the π–π stacking (020) planes which are most important for the charge transport.[11] The postgrowth annealing can improve the edge-on oriented crystallites, but it is difficult to apply to devices prepared on flexible plastic substrate. It would be therefore interesting to slow down the kinetics of film growth to approach equilibrium conditions, e.g., by lowering the casting temperature of a P3HT film.

This work demonstrates the advantage of casting the P3HT films below room temperature (RT). The reduced solvent evaporation rate at low temperature enhances the crystallinity and preferential orientation of the crystalline domains on native and silanized substrates of $Si/SiO_2$. In addition, the annealing temperature and its duration have been determined as important factors to increase the average size of the crystalline domains and to enhance their orientation. Improvements in orientation and crystallinity of the drop-cast P3HT films were probed by X-ray diffraction and transmission electron microscopy (TEM).

## EXPERIMENTAL SECTION

High molecular weight (HMW) P3HT (76,400 and 46,500 g/mol; PDI is 1.52 and 1.47) has been synthesized at the University of Wuppertal, Germany. The cast films were prepared by depositing 250 μL of a 2-mg/mL solution of P3HT in $CHCl_3$ onto a 2.5 × 2.5 $cm^2$ clean substrates of Si(100) covered with 300-nm thick thermal oxide. The thicknesses of the films are found to be independent of growth temperature and about 400 nm as measured by atomic force microscopy (AFM). For TEM analysis, the concentration of the solution was reduced to 1 mg/12 mL to prepare ≈40-nm thick drop cast films. Before the deposition, the substrates were cleaned with diluted hellmanex®II (Hellma GmbH) and rinsed with 2-propanol, acetone, and distilled water. Some of the substrates were cleaned with hexane and 2-propanol which were initially coated with *n*-octadecyltrichlorosilane (OTS, Merck) as silanizing agent. During the casting protocol, the evaporation rate of the solvent as well as the supersaturation ratio of the solution was controlled by varying the casting temperature of the films in the range of 23 to −30°C. Before dropping the solution, both the substrate and solution were thermalized for nearly 10 min at the growth temperature (to avoid the temperature gradients). Three sets of cast films were annealed at 100, 150, and 200°C in a glass oven under primary vacuum (1 Torr).

The X-ray measurements were performed using two setups: (i) a Cu-tube source (high-resolution Seifert XRD 3003, λ = 1.54 Å) equipped with a point detector and (ii) a synchrotron radiation source (λ = 0.83 Å) at BL9 of DELTA, Dortmund, Germany with a two-dimensional (2D) image plate detector (MarCCD) kept 500 mm apart from the sample (the distance and the incidence angle were varied with respect to the wavelength). The incidence angle $\alpha_i$ (0.13° and 0.22° for DELTA and lab sources, respectively) was fixed slightly above the critical angle of the P3HT film to maximize the scattering signal. The line scans were recorded over a large range of diffraction angles (2θ) with a step size of 0.02° using Cu tube source. The exposure time of the image plate detector was varied between 3 and 20 min depending on the scattering intensity. *In situ* annealing analysis was performed using an Anton Paar DHS 900 (heating stage). While increasing the temperature at a rate of 10°C/min, the (100) diffraction peak shifted to smaller scattering angles due to the lattice expansion. Once the desired temperature was reached, the peak intensity was recorded every 10 s.

TEM analysis was carried out using a CM12 Philips microscope at 120 kV equipped with a MVIII CCD camera in both electron diffraction (ED) and Bright field (BF) modes. For TEM analysis, P3HT films were coated with an amorphous carbon layer. The carbon-coated film were subsequently lift up from the $SiO_2$ substrate by dipping the films in an 5-Wt % aqueous HF solution and recovered on TEM copper grids. Calibration of the ED patterns was performed by using an oriented poly(tetrafluoroethylene) film. Intensity plot profiles were extracted from the ED patterns by angular averaging using the appropriate macro routine of ImageJ (National Institute of Health).

## RESULTS AND DISCUSSION

The X-ray diffraction analysis was performed under grazing incidence geometry as schematically shown in Figure 1(f). The relation between the $Q$ and $Q_{x,y}$ reciprocal space coordinates corresponding to the

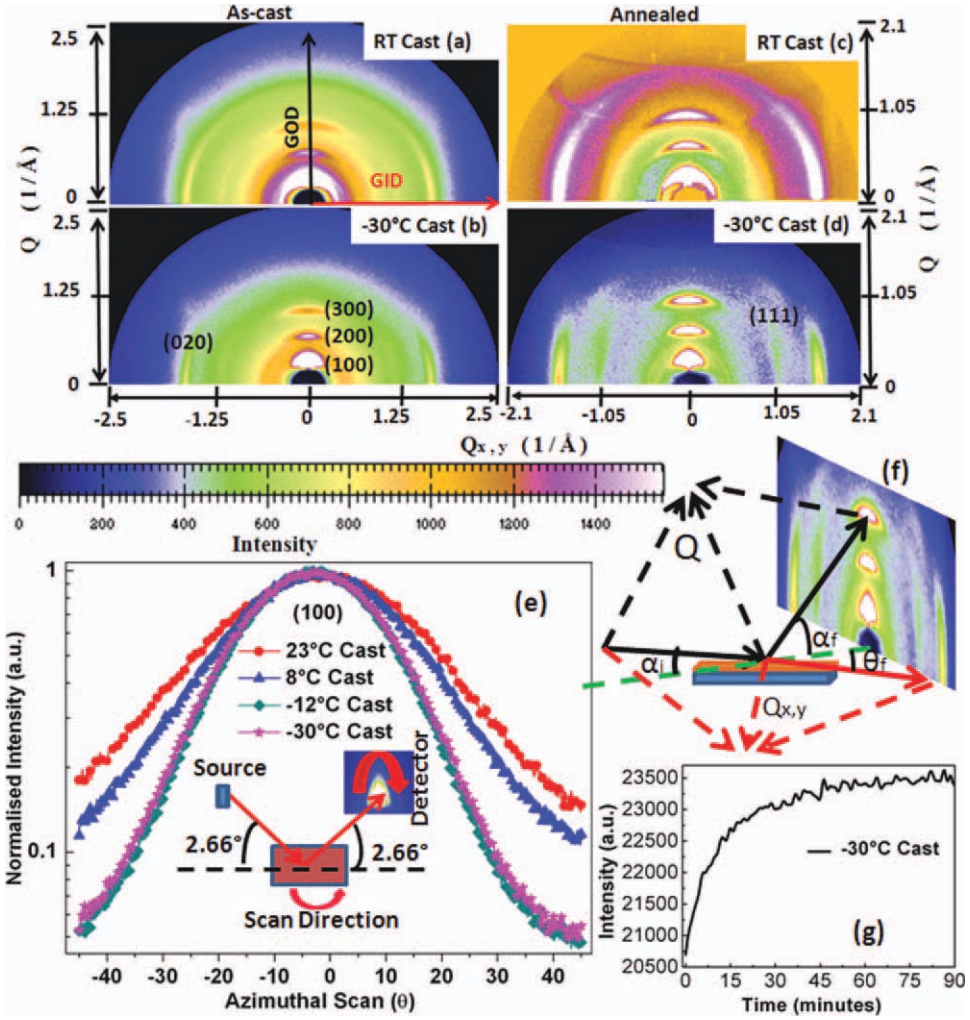


**Figure 1** Two-dimensional (2D) GIXD patterns of the RT (a) and −30°C (b) as-cast films and the corresponding (c) and (d) 185°C annealed films; (e) azimuthal intensity distribution of different temperature as-cast films normalized to one and its geometrical scheme is in inset; (f) schematic illustration of GIXD; (g) the enhancement in intensity of (100) GOD Bragg peak during annealing (1.5 h) at 200°C. [Color figure can be viewed in the online issue, which is available at wileyonlinelibrary.com.]

out-of- and in-plane (GOD and GID) probing directions can be found elsewhere.[11] The acquired 2D X-ray diffraction patterns are shown in Figure 1(a–d). Figure 1(a,b) shows the diffraction pattern of RT and −30°C as-cast P3HT films. The same films are shown in Figure 1(c,d) which underwent 1 h of annealing at 185°C. All the diffraction patterns exhibit a series of (h00) reflections along $Q$ and less intense (020) peak along $Q_{x,y}$ suggesting the growth of preferentially edge-on oriented crystallites but the fraction of face-on oriented crystallites is observed in the RT cast films [Fig. 1(a,c)]. For the better visualization, a line profile was taken along in-plane direction and shown in Supporting Information Figure S1. The (020) peak typically refers to the interchain π–π stacking distance (3.8 Å), whereas the (out-of-plane (h00)) interplanar distance (16.7 Å) associated with hexyl side chains. X-Ray measurements of both the MW P3HTs, e.g., 76,400 and 46,500 g/mol provide same $d_{(100)}$-spacing similar to the $CHCl_3$ fraction of deuterated P3HT as observed by A. Zen et al.[14] Almost all studies were performed using the 76,400 g/mol P3HT except of the *in situ* annealing analysis [Fig. 1(g)] and the 2D patterns of 185°C annealed films [Fig. 1(c,d)]. Similar to the d-spacing, we did not observe much variation in the scattering patterns of different MW fraction as observed by Kline et al.[5] In contrast to the RT cast film, the scattering pattern of the film cast at −30°C [Fig. 1(b)] consists of intense and narrow (h00) and (020) peaks along $Q$ and $Q_{x,y}$ directions, respectively. The presence of the (111) Bragg peak underlines the enhanced crystalline perfection of the domains while casting at −30°C [Fig. 1(d)]. Qualitatively, the 2D images of the films grown at −30 and −12°C exhibit similar scattering patterns. The annealing duration was optimized by probing the evolution of the (100) peak intensity as a function of annealing time at

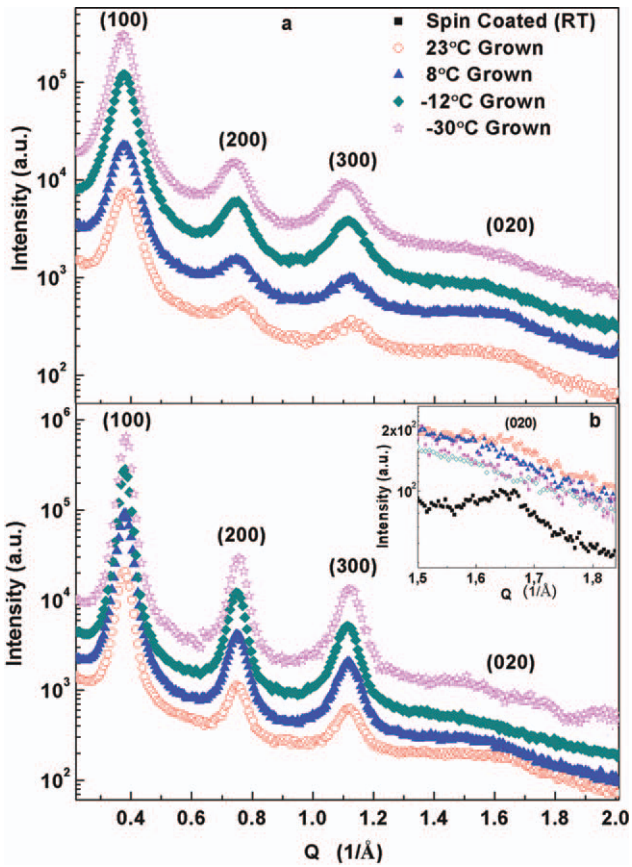


**Figure 2** (a) GOD profiles of as-cast and (b) 200°C annealed samples probed by a point detector; the graphs were shifted by multiplying some factors for the clear view from the same baseline. [Color figure can be viewed in the online issue, which is available at wileyonlinelibrary.com.]

200°C, it tends to saturate after 30 min [Fig. 1(g)]. Therefore, the crystallinity cannot be further enhanced by increasing the annealing duration. After annealing, the (h00) and (020) diffraction peaks [Fig. 1(c,d)] become narrower and more intense as compared to the as-grown films.

To quantify the azimuthal distribution of the nanocrystallites, the as-cast films were rotated between $\theta = \pm 45°$ at the fixed Bragg condition ($\alpha_i = \alpha_f = \theta_B$) of the (100) Bragg peak [see scheme in inset of Fig. 1(e)]. The azimuthal profiles [Fig. 1(e)] visualizes the anisotropic orientational distribution of the crystallites with the full width at half maximum (FWHM) of about 26° for the −30 and −12°C cast films. A clear trend is observed: the FWHM increases with increase of casting temperature, e.g., 31° at 8°C and 34° at 23°C.

The line scans along in- and out-of-plane directions were performed to compare the enhancement in crystallinity of the film as indicated in Figure 1(a) by red and black arrows. The obtained GOD line scans are shown in Figure 2, the as-grown and annealed films are displaying a series of (h00) peaks with an only broad and ill-defined hump at the position of (020) peak. Figure 2(a) reveals a strong increase of the (h00) peak intensities while lowering the cast temperature. The enhancement in (h00) peak intensities has been observed together with the reduction in FWHM after annealing at 200°C [see Fig. 2(b)]. Moreover, a broad hump centered in the (020) peak position is only visible for the RT, 8°C cast and RT spin-coated film [inset Fig. 2(b) black color] which is attributed to the presence of amorphous as well as face-on oriented P3HT fractions. Overall, these results demonstrate that the highly crystalline P3HT films can be prepared by lowering the cast temperature. This is further substantiated by the evolution of the (100) Bragg peak intensity and the crystallite size estimated by Scherrer's equation[15] as shown in Figure 3(a,b) for different annealing temperatures. The influence of casting temperature on the crystallite orientation can be qualitatively estimated by comparing the integrated intensities of (100) Bragg peak because the thickness of the films used for the analysis are comparable. The (100) peak intensity of the −30°C cast film is four times larger than the RT-cast film whereas the crystallite

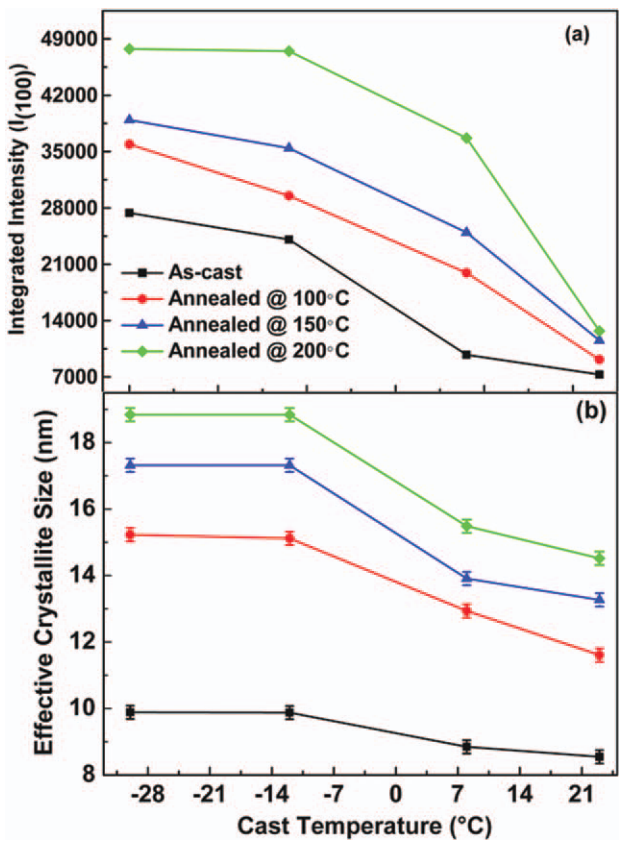


**Figure 3** (a) Variation in integrated intensity of the first-order Bragg peak [I(100)] and (b) the effective crystallite size depending on the growth and annealing temperatures. [Color figure can be viewed in the online issue, which is available at wileyonlinelibrary.com.]

**TABLE I**
**The Influence of Annealing Temperature on the Effective Crystallite Size of P3HT Thin Films Cast at Different Temperatures**

| Cast temperature (°C) | Effective crystallite size (±0.2 nm) on | | | |
|---|---|---|---|---|
| | | Annealing temperature (°C) | | |
| | As-cast | 100 | 150 | 200 |
| 23 | 8.5 | 11.6 | 13.2 | 14.5 |
| 8 | 8.8 | 12.9 | 13.9 | 15.5 |
| −12 | 9.8 | 15.1 | 17.3 | 18.9 |
| −30 | 9.9 | 15.2 | 17.3 | 18.9 |

size does not increase much (increases by ≈1.5 nm compared to RT cast one). The crystallite size is increased by a factor of about two after annealing at 200°C. It gradually increases with increasing the annealing temperature (Table I). This result suggests that both the number of edge-on oriented crystallites and the crystallite size increases with decreasing the cast temperature. The cast temperature $T \approx -12$°C can be assumed as the optimum crystallization temperature, because there is no major enhancement in both the quantities by further reduction of growth temperature [Fig. 2(a,b)]. The orientation of the crystallites can be further enhanced by casting the films onto an OTS-treated substrate. For the RT and −30°C cast films, one observes a gain in diffracted intensity of the (100) peak by a factor 2 and 6, respectively, when compared with the non-OTS-treated samples (Supporting Information Fig. S2).

Complementary to the X-ray diffraction, ED analysis was performed to visualize the in-plane ordering of the films [Fig. 4(a,b)]. All the ED patterns are composed by a number of Scherrer rings with variable intensities. Figure 4(e) shows the corresponding intensity profiles obtained after angular averaging. As observed in the X-ray diffraction [Supporting Information Fig. S2 and inset Fig. 2(b)], the spin-coated film [Fig. 4(e)] show the coexistence of weak (h 00) ($h = 1$, 2, and 3) and (020) reflections confirming the absence of preferential orientation of crystalline domains on the $SiO_2$ substrate, i.e., face-on and edge-on domains seem to coexist. In contrast to this, the diffraction profiles of −30°C cast film does not show any (h00) reflections and most of the observed reflections are indexed as (0k0) and (0kl) using the structure of P3HT reported by Kayunkid et al.[16] The presence of these mixed b- and c-reflections, especially, the (011) reflection at $Q = 1.18$ Å$^{-1}$ is an indication for the higher crystalline perfection of the domains in the −30°C cast films.

In addition to the diffraction data, BF images were acquired to observe the impact of casting temperature on the resulting film morphology. [Fig. 4(c,d)]. To visualize the nanomorphology by BF contrast, both a small objective aperture and adequate defocusing were necessary to enhance the contrast between the crystalline and amorphous domains in the films. The P3HT film obtained by RT casting exhibits a distribution of elongated nanofibrils with a characteristic length below 200 nm and a typical width of 15–20 nm. This morphology is reminiscent of the long nanofibrils observed by AFM in spin-coated or drop cast P3HT films.[17,18] The morphology of the −30°C cast films turns out to be very different. Instead of nanofibrils, the BF shows an assembly of lamellar crystals separated by the bright contour lines corresponding most presumably to the "grain boundaries" between the lamellae. Contrary to the highly oriented P3HT films grown by epitaxy on the substrates of potassium 4-bromo-benzoate, no clear nanomorphology corresponding to the amorphous/crystalline alternation could be observed in the domains of drop cast P3HT.[9] This observation supports the GIXD results, i.e., that the −30°C cast film are composed of mainly edge-on oriented crystallites (Fig. 5).

The growth of highly crystalline and oriented thin films of polymeric semiconductors like P3HT have been identified as an essential prerequisite for the preparation of OFETs with improved charge transport.[1,5–8] Our X-ray and electron diffraction results gathered in this study shows that the highly crystalline HMW P3HT thin films with preferential edge-on orientation of the conjugated backbone can be prepared by drop casting $CHCl_3$ solutions at temperatures below 0°C (Fig. 5). The reduction in casting temperature of the P3HT solution has two important effects: (i) slowing down the evaporation rate of $CHCl_3$, i.e., the kinetics of P3HT aggregation and (ii) lowering the P3HT concentration at supersaturation. At RT, the fast evaporation of $CHCl_3$ leads to kinetically trapped morphologies far from equilibrium with reduced domain sizes. Instead, at −30°C, solvent evaporation is slow, and hence, the aggregation occurs on a longer time scale that allows polymer chains to find the thermodynamically most stable position in an aggregate and also to adopt the most favorable orientation of the domains with respect to the substrate (Fig. 5).

In terms of crystallinity, low-temperature casting provides analogous results to the use of solvents with higher boiling points.[10] However, from the technological point of view, the low-temperature casting protocol might be advantageous, because it is less costly due to low consumption of material and more environmental friendly. The diluted P3HT solution (1 mg of P3HT dissolved in 14 mL of $CHCl_3$) can provide thin and rather uniform film via casting at low temperature (−30°C) which is not possible to achieve by casting at RT, but the selection of appropriate concentration and cast

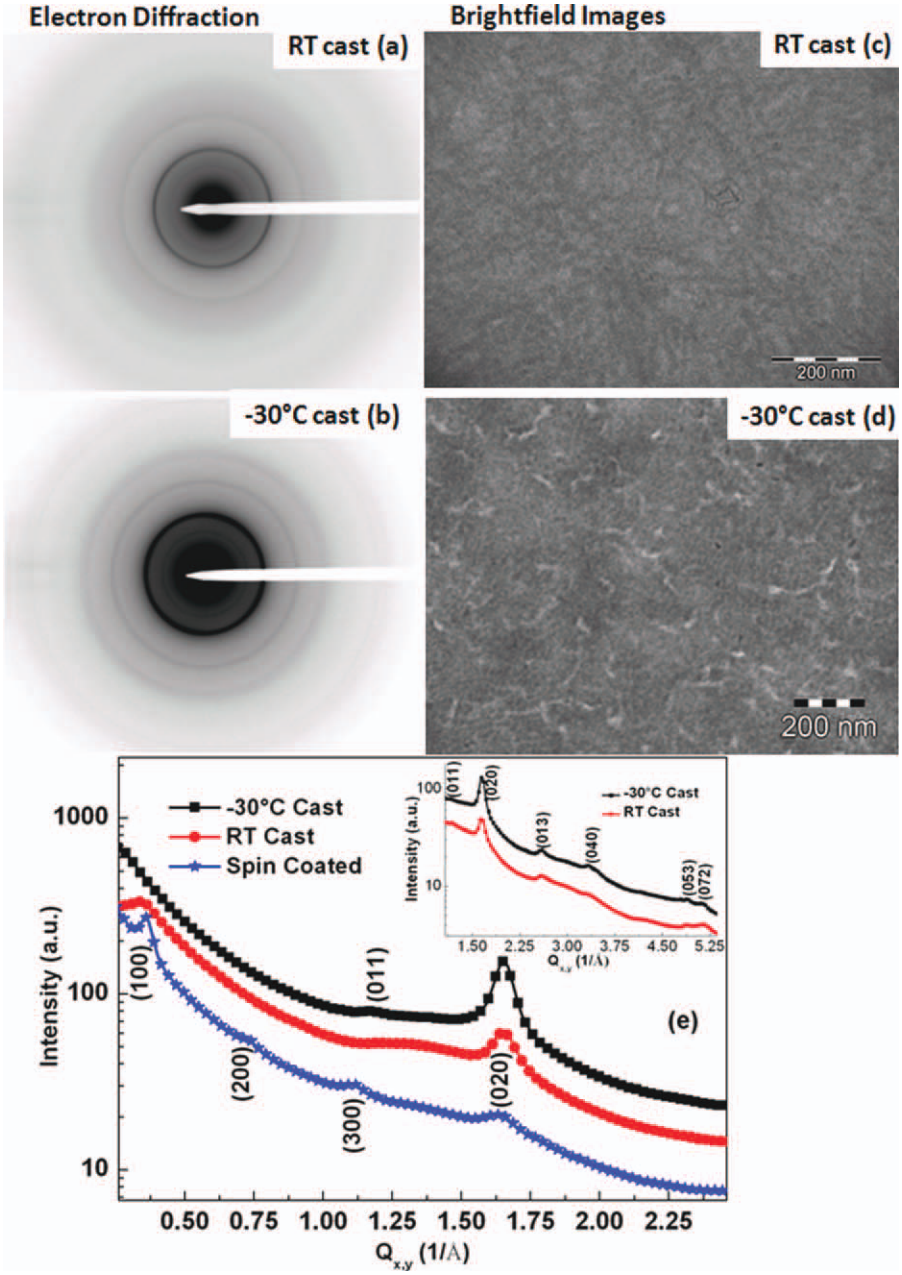


**Figure 4** (a) Electron diffraction pattern of RT and (b) −30°C cast films; (c) and (d) shows theirs corresponding BF images; (e) the angular averaging of ED pattern of different condition grown P3HT thin films plotted versus $Q$-space ($Q_{x,y}$) (the profiles were shifted by multiplying some factor from the same baseline). [Color figure can be viewed in the online issue, which is available at wileyonlinelibrary.com.]

temperatures are mandatory. The temperature-dependent measurement reveals that the optimum growth temperature is close to −12°C which is technologically straightforward to achieve. Further reduction in the growth temperature does not increase significantly the thin film crystallinity for a given concentration (2 mg/mL). This study additionally demonstrates that crystallinity and preferential orientation of P3HT nanocrystallites can be improved by low-temperature casting on OTS-treated $SiO_2$ substrates as observed in previous reports.[5,11,19] The proper choice of annealing temperature can further help to improve the crystallinity of the films [see Figs. 1(g), 2(b), and 3] due to further ripening of the crystalline nanodomains and reorientation of the crystallites.[20]

## CONCLUSIONS

Finally, we have shown that the highly crystalline high molecular weight P3HT thin films can be fabricated by low-temperature drop-casting. Casting is a

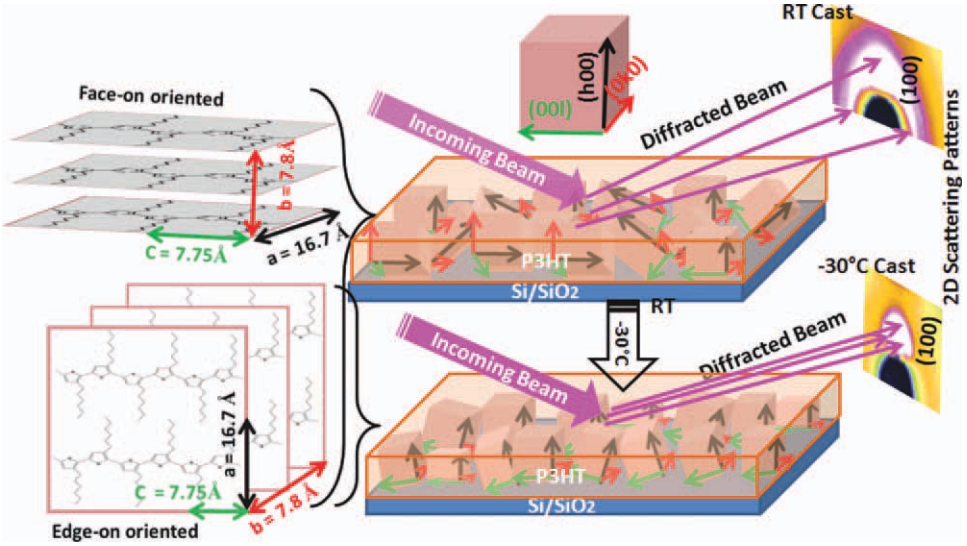


**Figure 5** Schematically illustrate the formation of edge-on oriented crystallites due to the reduction in growth temperature which can prolong the growth time. [Color figure can be viewed in the online issue, which is available at wileyonlinelibrary.com.]

low-cost fabrication method of large-scale devices although it suffers from fluctuation in density and layer thickness across the film. As compared to casting, the spin-coating technique leads to uniform thin films but engenders large wastes of polymer material and does not allow for a precise control of the face-on versus edge-on orientation of the crystallites, which hampers to a certain extent the OFET performances.. These drawbacks have been overcome by low-temperature casting which provides a route to enhance the orientation, crystallinity, and uniformity of thin films by varying the solution concentration and growth temperature. Further on, low-temperature casting protocols may be extended to the printing and doctor blade methods to produce low-cost electronic devices with highly crystalline and edge-on oriented P3AT thin films. In particular, the low-temperature casting method would be suited to the elaboration of OFETs on flexible polymeric substrates that cannot undergo high-temperature annealing steps. In addition, as compared to the conventional spin coating, the low-temperature casting method consumes far less polymer and this can potentially help to reduce the corresponding manufacturing cost.

The authors are thankful to BL9 beamline staff at DELTA, Dortmund, for experimental support.

## References

1. Wong, W. S.; Salleo, A. Flexible Electronics: Materials and Applications; Springer: New York, 2009.
2. Krebs, F. C. Solar Energy Mater Solar Cells 2009, 93, 394.
3. Sauve, G.; Javier, A. E.; Zhang, R.; Liu, J.; Sydlik, S. A.; Kowalewski, T.; McCullough, R. D. J Mater Chem 2010, 20, 3195.
4. Friedel, B.; McNeill, C. R.; Greenham, N. C. Chem Mater 2010, 22, 3389.
5. Kline, R. J.; McGehee, M. D.; Toney, M. F. Nat Mater 2006, 5, 222.
6. Salleo, A.; Kline, R. J.; DeLongchamp, D. M.; Chabinyc, M. L. Adv Mater 2010, 22, 3812.
7. Sirringhaus, H.; Brown, P. J.; Friend, R. H.; Nielsen, M. M.; Bechgaard, K.; Langeveld-Voss, B. M. W.; Spiering, A. J. H.; Janssen, R. A. J.; Meijer, E. W.; Herwig, P.; Leeuw, D. M. de. Nature 1999, 401, 685.
8. Jimison, L. H.; Toney, M. F.; McCulloch, I.; Heeney, M.; Salleo, A. Adv Mater 2009, 21, 1568.
9. Brinkmann, M.; Contal, C.; Kayunkid, N.; Djuric, T.; Resel, R. Macromolecules 2010, 43, 7604.
10. Chang, J. F.; Sun, B.; Breiby, D. W.; Nielsen, M. M.; Sölling, T. I.; Giles, M.; McCulloch, I.; Sirringhaus, H. Chem Mater 2004, 16, 4772.
11. Joshi, S.; Pingel, P.; Grigorian, S.; Panzner, T.; Pietsch, U.; Neher, D.; Forster M.; Scherf, U. Macromolecules 2009, 42, 4651.
12. Wang, T.; Dunbar, A. D. F.; Staniec, P. A.; Pearson, A. J.; Hopkinson, P. E.; MacDonald, J. E.; Lilliu, S.; Pizzey, C.; Terrill, N. J.; Donald, A. M.; Ryan, A. J.; Jones, R. A. L.; Lidzey, D. G. Softmatter 2010, 6, 4128.
13. Chabinyc, M. L.; Toney, M. F.; Kline, R. J.; McCulloch, I.; Heeney, M. J Am Chem Soc 2007, 129, 3226.
14. Zen, A.; Saphiannikova, M.; Neher, D.; Grenzer, J.; Grigorian, S.; Pietsch, U.; Asawapirom, U.; Janietz, S.; Scherf, U.; Lieberwirth, I. Macromolecules 2006, 39, 2162.
15. Warren, B. E. X-Ray Diffraction, Dover Publications, Inc.: New York, 1990.
16. Kayunkid, N.; Uttiya, S.; Brinkmann, M. Macromolecules 2010, 43, 4961.
17. Kline, R. J.; McGehee, M. D.; Kadnikova, E. N.; Liu, J.; Frechet, J. M. J.; Toney, M. F. Macromolecules 2005, 38, 3312.
18. Yang, H.; LeFevre, S. W.; Ryu, C. Y. Appl Phys Lett 2007, 90, 172116.
19. Choi, D.; Jin, S.; Lee, Y.; Kim, S. H.; Chung, D. S.; Hong, K.; Yang, C.; Jung, J.; Kim, J. K.; Ree, M.; Park, C. E. Appl Mater Interfaces 2010, 2, 48.
20. Jimison, L. H.; Salleo, A.; Chabinyc, M. L.; Bernstein, D. P.; Toney, M. F. Phys Rev B 2008, 78, 125319.